Supporting information for:

Structure prediction of mixed-anion perovskites: systematic approach integrating octahedral tilting and anion ordering

Sanni Määttänen and Antti J. Karttunen

Department of Chemistry and Materials Science, Aalto University, P.O. Box 16100, FI-00076 Aalto, Finland.
E-mail: antti.karttunen@aalto.fi

Table S1. Detailed listing of the anion distributions in a mixed-anion ABX_2Y perovskite.

Tilt system	Space group	Anion Wyckoff positions	Number of different anion distributions	Distributions of anion Y on the Wyckoff positions	Ordered structures for each anion distribution
1	204 $Im\bar{3}$	24*g*	1	8 Y anions on site 24*g*	16 000
2	137 $P4_2/nmc$	8*g* 8*g* 8*f*	45	1:1:6 (8*g*:8*g*:8*f*)	120
				1:2:5	784
				1:3:4	1 996
				1:4:3	1 960
				1:5:2	808
				1:6:1	112
				1:7:0	6
				1:0:7	4
				8:0:0	1
				2:1:5	784
				2:2:4	3 548
				2:3:3	5 488
				2:4:2	3 552
				2:5:1	784
				2:6:0	66
				2:0:6	64
				3:1:4	1 996
				3:2:3	5 488
				3:3:2	5 560
				3:4:1	1 960
				3:5:0	214
				3:0:5	196
				4:1:3	1 960
				4:2:2	3 552
				4:3:1	1 960
				4:4:0	352
				4:0:4	344
				5:1:2	808
				5:2:1	784
				5:3:0	214
				5:0:3	196
				6:1:1	112
				6:2:0	66
				6:0:2	64
				7:1:0	6
				7:0:1	4
				0:1:7	4
				0:2:6	64
				0:3:5	196
				0:4:4	344
				0:5:3	196
				0:6:2	64
				0:7:1	4
				0:8:0	1
				0:0:8	1
3	62 *Pnma*	4*c* 8*d*	5	0:4	854
				1:3	14 252
				2:2	8 192
				3:1	224
				4:0	1
4	15 *C*2/*c*	4*e* 8*f*	5	0:4	854

				1:3	14 196
				2:2	8 108
				3:1	236
				4:0	1
5	167 $R\bar{3}c$	18*e*	1	6	555
6	139 *I4/mmm*	8*h* 16*f*	9	0:8	490
				1:7	2 860
				2:6	7 344
				3:5	7 644
				4:4	4 248
				5:3	980
				6:2	114
				7:1	4
				8:0	1
7	63 *Cmcm*	8*e* 8*f* 8*g*	45	1:1:6	112
				1:2:5	784
				1:3:4	1960
				1:4:3	1960
				1:5:2	784
				1:6:1	112
				1:7:0	4
				1:0:7	4
				8:0:0	1
				2:1:5	784
				2:2:4	3656
				2:3:3	5488
				2:4:2	3656
				2:5:1	784
				2:6:0	76
				2:0:6	76
				3:1:4	1960
				3:2:3	5488
				3:3:2	5488
				3:4:1	1960
				3:5:0	196
				3:0:5	196
				4:1:3	1960
				4:2:2	3656
				4:3:1	1960
				4:4:0	388
				4:0:4	388
				5:1:2	784
				5:2:1	784
				5:3:0	196
				5:0:3	196
				6:1:1	112
				6:2:0	76
				6:0:2	76
				7:1:0	4
				7:0:1	4
				0:1:7	4
				0:2:6	76
				0:3:5	196
				0:4:4	388
				0:5:3	196
				0:6:2	76
				0:7:1	4

				0:8:0	1
				0:0:8	1
8	74 *Imma*	4*e* 8*f*	5	0:4	490
				1:3	7 344
				2:2	4 248
				3:1	144
				4:0	1
9	127 *P4/mbm*	2*a* 4*h*	3	0:2	440
				1:1	4 076
				2:0	1
10	40 *I*4/*mcm*	4*a* 8*h*	5	0:4	283
				1:3	3 796
				2:2	2 222
				3:1	84
				4:0	1
11	221 $Pm\bar{3}m$	3*c*	1	1	2664

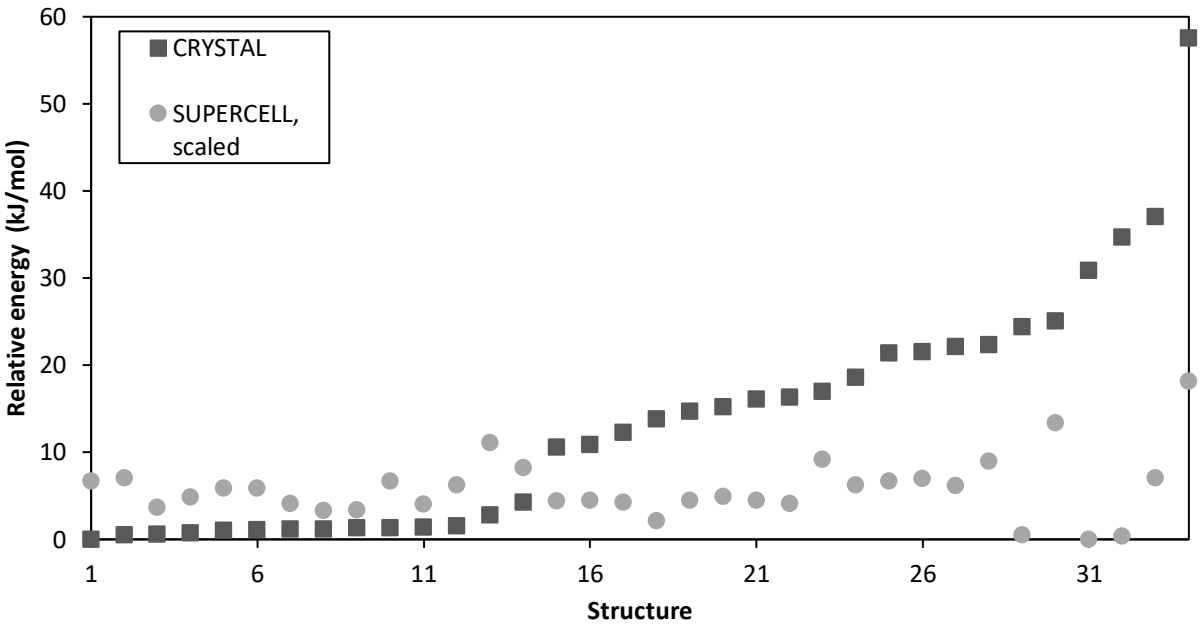

Figure S1. Relative DFT-PBE0 energies (CRYSTAL) and relative SUPERCELL Coulomb energies for 34 anion-ordered $SrTaO_2N$ structures (tilt system 10). For better comparison, the SUPERCELL energies have been scaled to the same energy scale. The *x*-axis shows the structures in increasing order of their DFT-PBE0 relative energies.

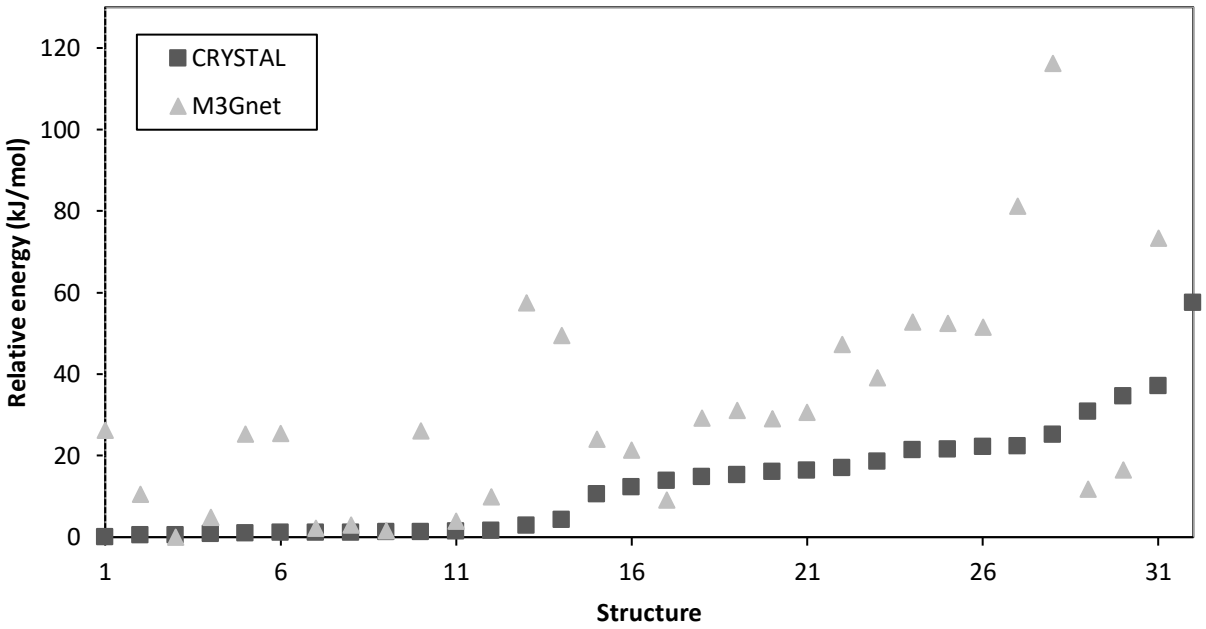

Figure S2. Relative DFT-PBE0 energies (CRYSTAL) and relative M3Gnet energies for 32 anion-ordered $SrTaO_2N$ structures (tilt system 10). The *x*-axis shows the structures in increasing order of their DFT-PBE0 relative energies.

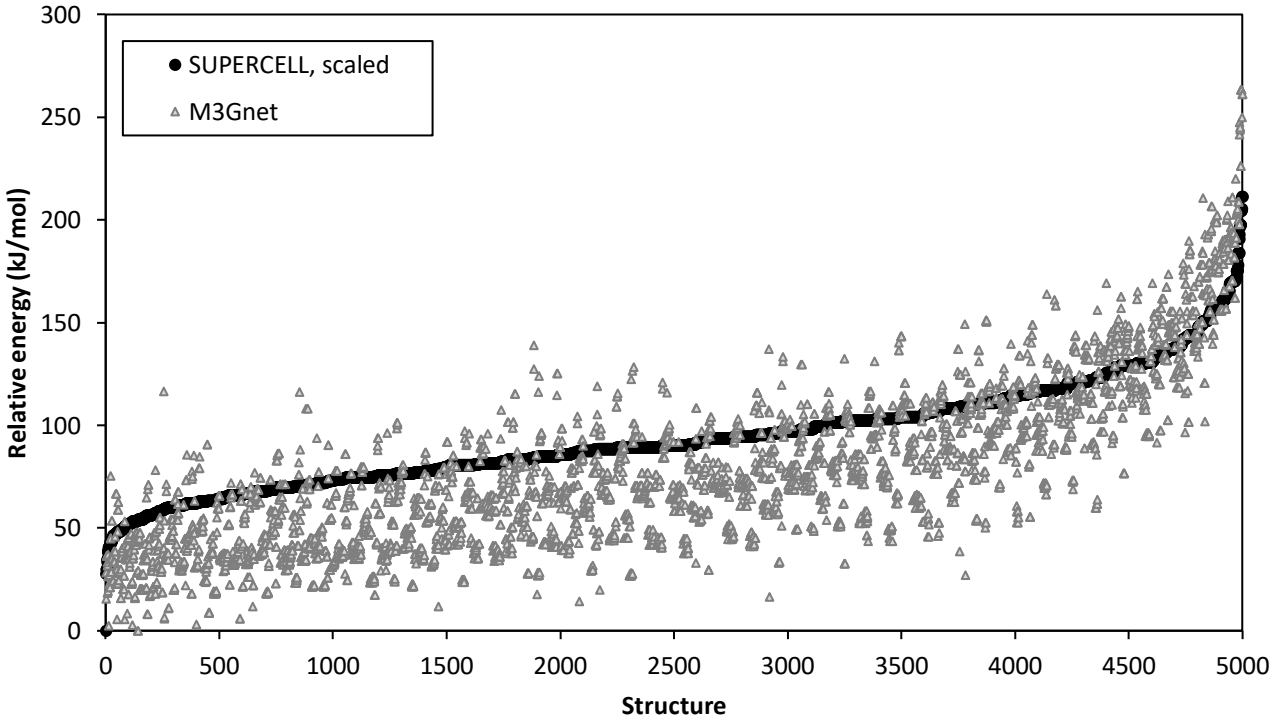

Figure S3. Relative SUPERCELL Coulomb energies and M3Gnet relative energies for 5 000 anion-ordered $BaTaO_2N$ structures (tilt system 1). For better comparison, the SUPERCELL energies have been scaled *to the same energy scale*. The *x*-axis shows the structures in the order of increasing SUPERCELL Coulomb energies.

Table S2. Reaction equations used for energy comparisons with respect to experimentally known phases. Oxidation states of metal atoms are listed after the reaction equations. Anions are always F(−I), O(−II), and N(−III)

$2\ MoO_3\ (s) + \ K_3MoN_3\ (s) \rightarrow 3\ KMoO_2N\ (s)$	Mo(VI), K(I)
$2\ MoO_3\ (s) + \ Na_3MoN_3\ (s) \rightarrow 3\ NaMoO_2N\ (s)$	Mo(VI), Na(I)
$YN\ (s) + TiO_2\ (s) \rightarrow YTiO_2N\ (s)$	Y(III), Ti(IV)
$KF\ (s) + ZrO_2\ (s) \rightarrow KZrO_2F\ (s)$	Zr(IV), K(I)
$NaF\ (s) + TiO_2\ (s) \rightarrow NaTiO_2F\ (s)$	Ti(IV), Na(I)
$SrO\ (s) + ScOF\ (s) \rightarrow SrScO_2F\ (s)$	Sc(III), Sr(II)
$KF\ (s) + ScOF\ (s) \rightarrow KScF_2O\ (s)$	Sc(III), K(I)
$KF\ (s) + YOF\ (s) \rightarrow KYF_2O\ (s)$	Y(III), K(I)
$NaF\ (s) + ScOF\ (s) \rightarrow NaScF_2O\ (s)$	Sc(III), Na(I)
$BaF_2\ (s) + BaN_2\ (s) + 2\ NbN\ (s) \rightarrow 2\ BaNbN_2F\ (s)$	Nb(III) → Nb(V), Ba(II)
$LaN\ (s) + ZrNF\ (s) \rightarrow LaZrN_2F\ (s)$	Zr(IV), La(III)
$BaF_2\ (s) + ScN\ (s) \rightarrow BaScF_2N\ (s)$	Sc(III), Ba(II)
$KF\ (s) + ZrNF\ (s) \rightarrow KZrF_2N\ (s)$	Zr(IV), Ba(II)
$KF\ (s) + TiNF\ (s) \rightarrow KTiF_2N\ (s)$	Ti(IV), K(I)

ICSD codes and references for reactions listed above:

Compound	**ICSD code**	**Reference**
MoO_3	35076	L. Kihlborg, *Ark. Kemi*, 1963, **21**, 357-364.
K_3MoN_3	Derived from Na_3MoN_3	
Na_3MoN_3	67565	D. Ostermann, U. Zachwieja and H. Jacobs, *J. Alloy Compd.*, 1992, **190,** 137-140.
YN	37413	C. P. Kempter, N.H. Krikorian and J.C. McGuire, *J. Phys. Chem.*, 1957, **61**, 1237-1238.
TiO_2	202240	J.K. Burdett, T. Hughbanks, G.J. Miller, J.W.jr Richardson and J.V. Smith, *J. Am. Chem. Soc.*, 1987, **109**, 3639-3646.
KF	52241	G.J. Finch and S. Fordham, *P. Phys. Soc. Lond.*, 1936, **48**, 85-94.
ZrO_2	23928	G. Teufer, *Acta Crystallogr.*, 1962, **15**, 1187.
NaF	262837	Y. Shirako, Y.G. Shi, A. Aimi, D. Mori, H. Kojitani, K. Yamaura, Y. Inaguma and M. Akaogi, *J. Solid State Chem.*, 2012, **191,** 167-174.
SrO	148358	N.I.P. Ayu, F. Takeiri, T. Ogawa, A. Kuwabara, M. Hagihala, T. Saito, T. Kamiyama and G. Kobayashi, *Dalton T.*, 2023, **52**, 15420-15425.
ScOF	24112	B. Holmberg, *Acta Chem. Scand.*, 1966, **20**, 1082-1088.
YOF	184004	S.E. Dutton, D. Hirai and R.J. Cava, *Mater. Res. Bull.,* 2012, **47**, 714-718.
BaF_2	53980	W.P. Davey, *Phys. Rev.*, 1922, **3**, 248-251.

BaN_2	280681	G.V. Vajenine, G. Auffermann, Y. Prots, W. Schnelle, R.K. Kremer, A. Simon and R. Kniep, *Inorg. Chem.*, 2001, **40**, 4866-4870.
NbN	982	A.N. Christensen, *Acta Chem. Scand. A*, 1977, **37**,, 77-78.
LaN	423892	S.B. Schneider, D. Baumann, A. Salamat and W. Schnick, *J. Appl. Phys.* 2012, **111**, 1-6.
ZrNF	21049	W. Jung and R. Juza, *Z. Anorg. Allg. Chem.*, 1973, **399**, 129-147.
ScN	26948	K. Becker and F. Ebert, *Z. Phys*., 1925, **31**, 268-272.
TiNF	63200	C. Wuestefeld, T. Vogt, U. Loechner, J. Straehle and H. Fuess, *Angew. Chem.*, 1988, **100**, 1013.

Table S3. Relative energies of the lowest-energy ordered models in the lowest-energy tilt system of each compound.

Compound	Lowest-energy tilt system	Relative energies (kJ/mol)
$KMoO_2N$	Tilt 11	0.0 0.8 16.4
$NaMoO_2N$	Tilt 09	0.0 13.3 19.7
$YTiO_2N$	Tilt 03	0.0 16.6
$KZrO_2F$	Tilt 11	0.0 2.2 4.1
$NaTiO_2F$	Tilt 05	0.0 0.4 2.3
$SrScO_2F$	Tilt 10	0.0 0.1 0.4
$KScF_2O$	Tilt 05	0.0 0.9 1.8
KYF_2O	Tilt 05	0.0 0.6 0.7
$NaScF_2O$	Tilt 08	0.0 9.7 12.9
$BaNbN_2F$	Tilt 05	0.0 1.0
$LaZrN_2F$	Tilt 04	0.0 8.5 9.0
$BaScF_2N$	Tilt 01	0.0
$KTiF_2N$	Tilt 05	0.0 6.4 10.0
$KZrF_2N$	Tilt 05	0.0 5.1 7.9

Table S4. Bond length analysis and Mulliken partial charge analysis for the lowest-energy ordered model of each tilt system for all compounds (DFT-PBE0). The lowest-energy tilt system is always on the left. For both B-X and B-Y bonds the shortest and longest bonds are presented.

$KMoO_2N$

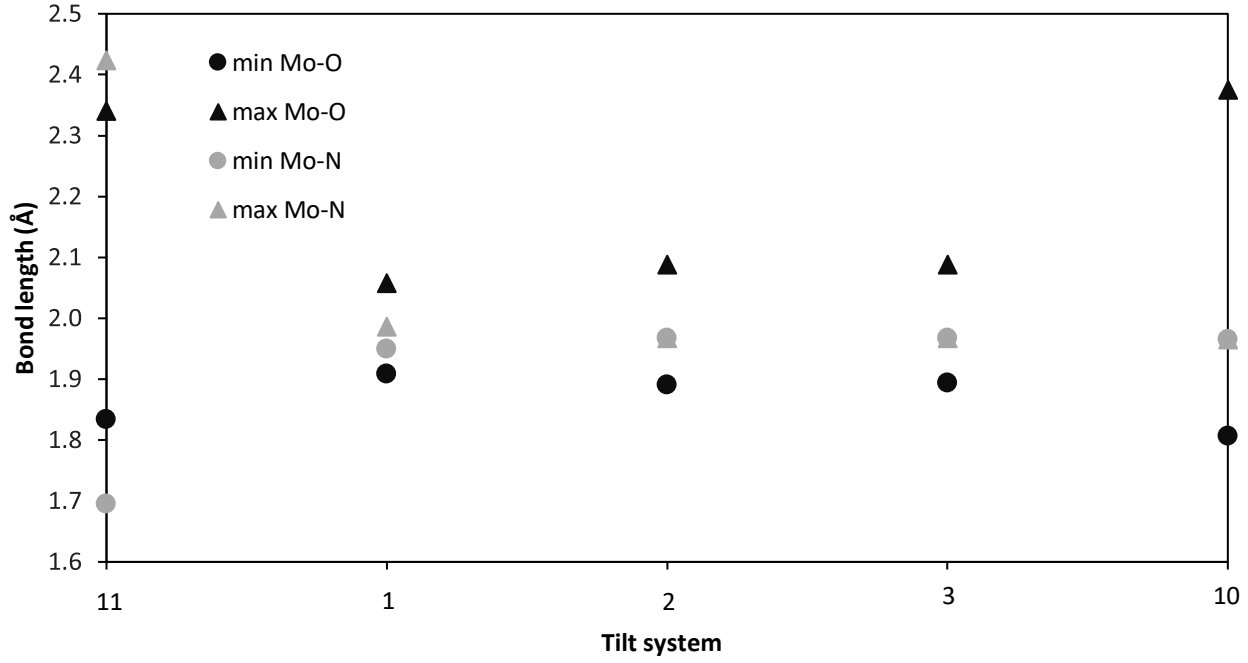

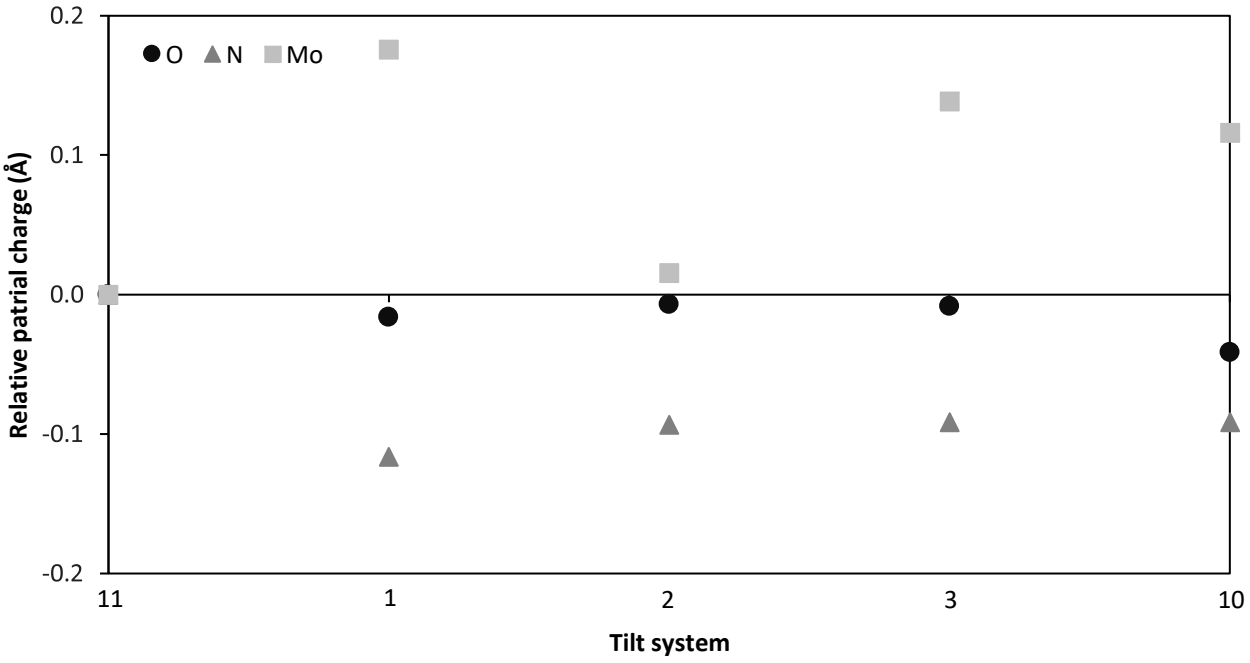

$KZrO_2F$

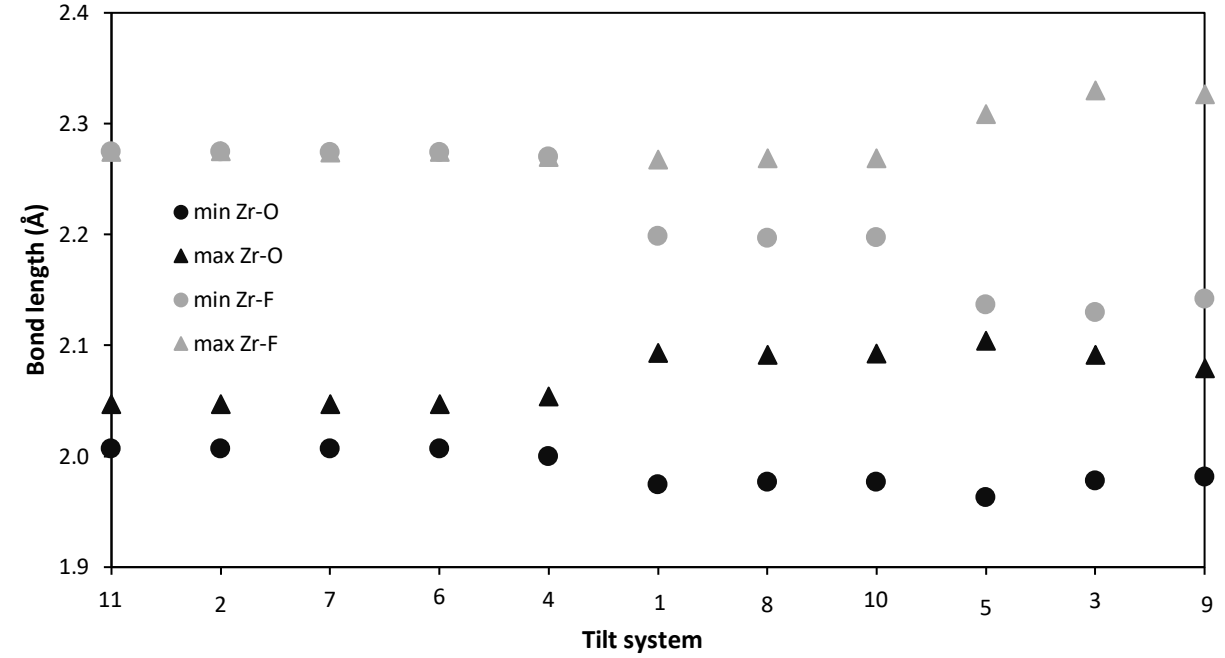
2.4
2.3
2.2
2.1
2.0
1.9
Bond length (Å)
min Zr-O
max Zr-O
min Zr-F
max Zr-F
11
2
7
6
4
1
8
10
5
3
9
Tilt system

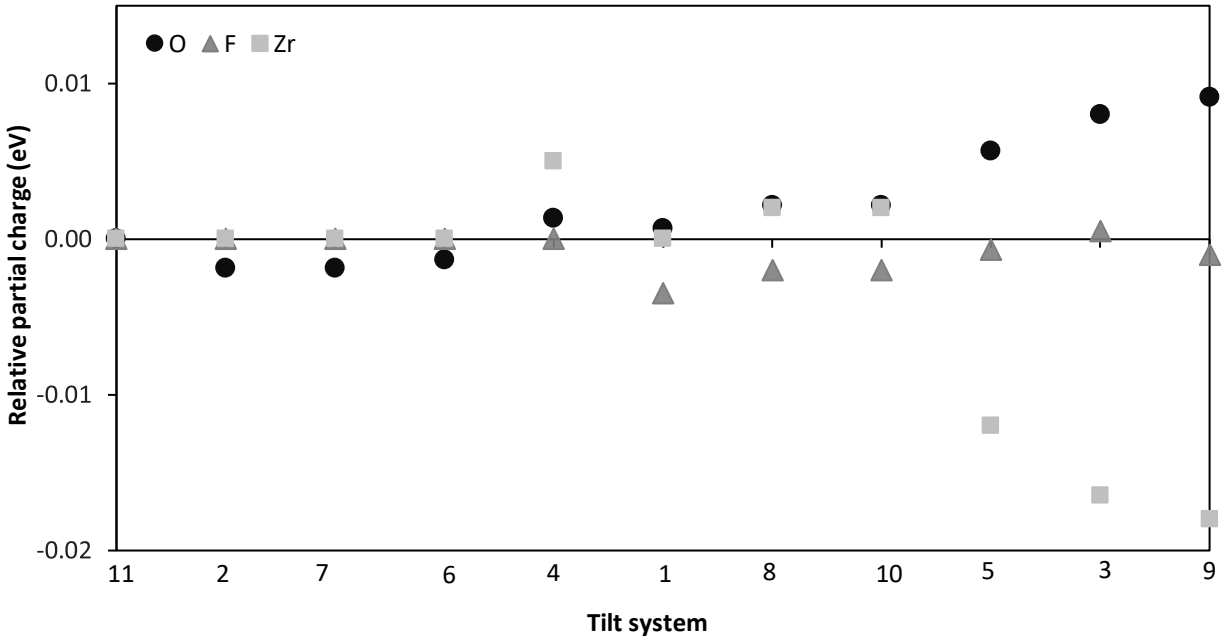
O
F
Zr
0.01
0.00
-0.01
-0.02
Relative partial charge (eV)
11
2
7
6
4
1
8
10
5
3
9
Tilt system

$NaTiO_2F$

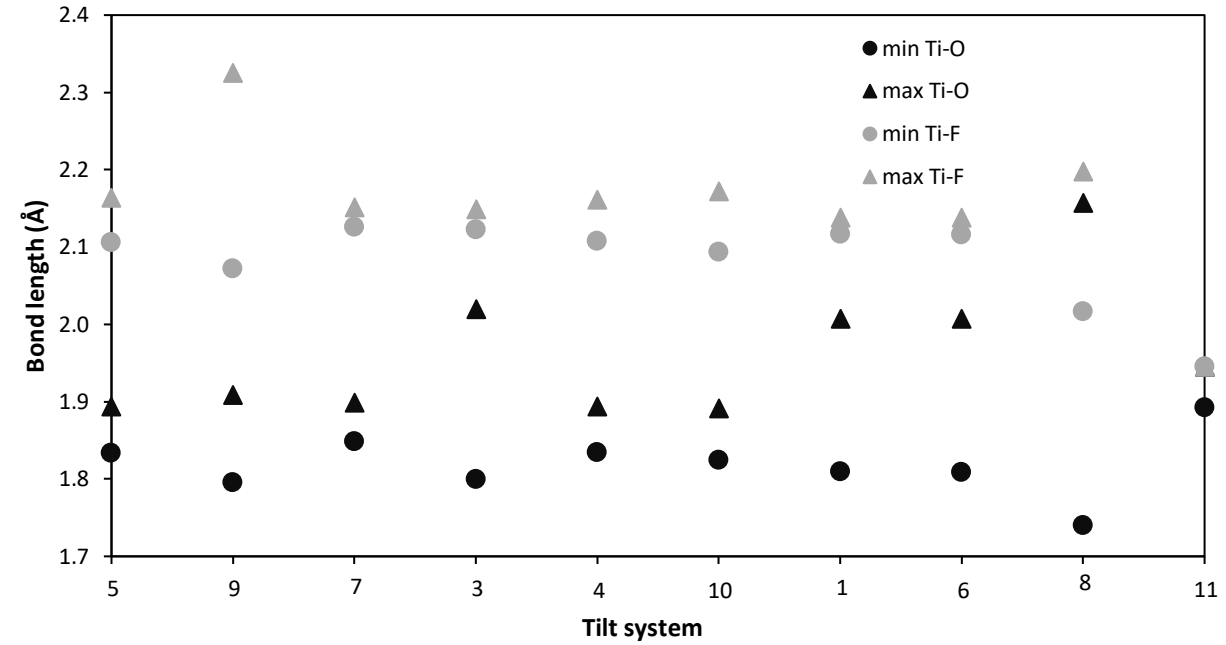
min Ti-O
max Ti-O
min Ti-F
max Ti-F
Bond length (Å)
2.4
2.3
2.2
2.1
2.0
1.9
1.8
1.7
5
9
7
3
4
10
1
6
8
11
Tilt system

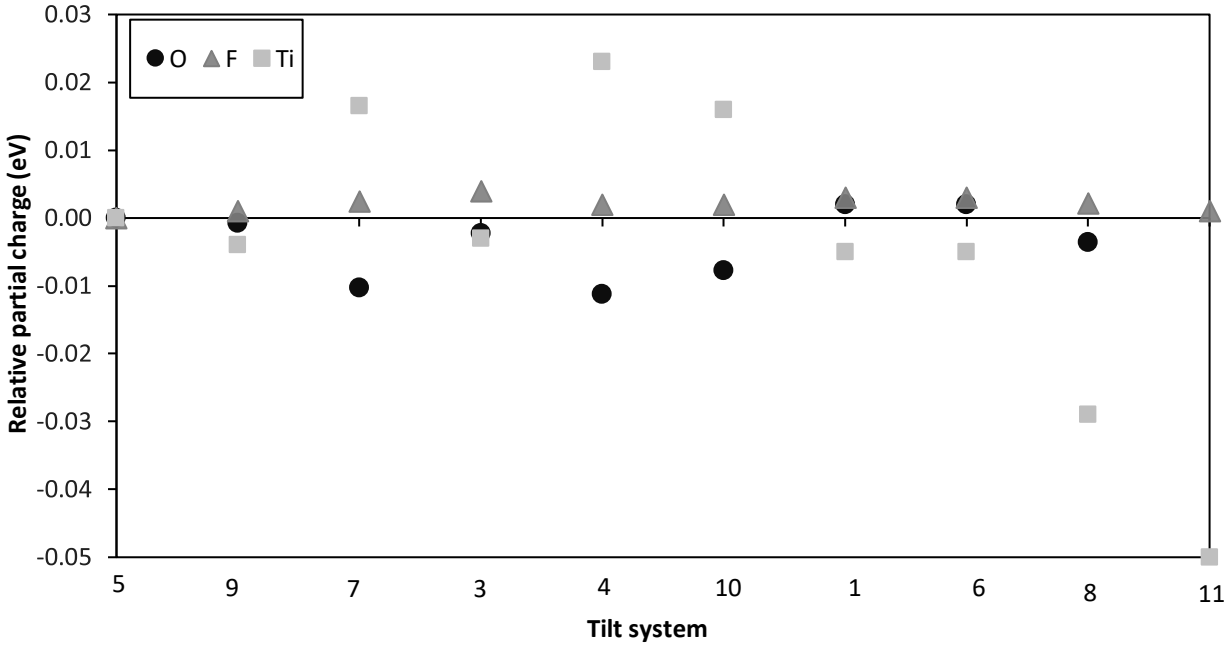
O
F
Ti
Relative partial charge (eV)
0.03
0.02
0.01
0.00
-0.01
-0.02
-0.03
-0.04
-0.05
5
9
7
3
4
10
1
6
8
11
Tilt system

$SrScO_2F$

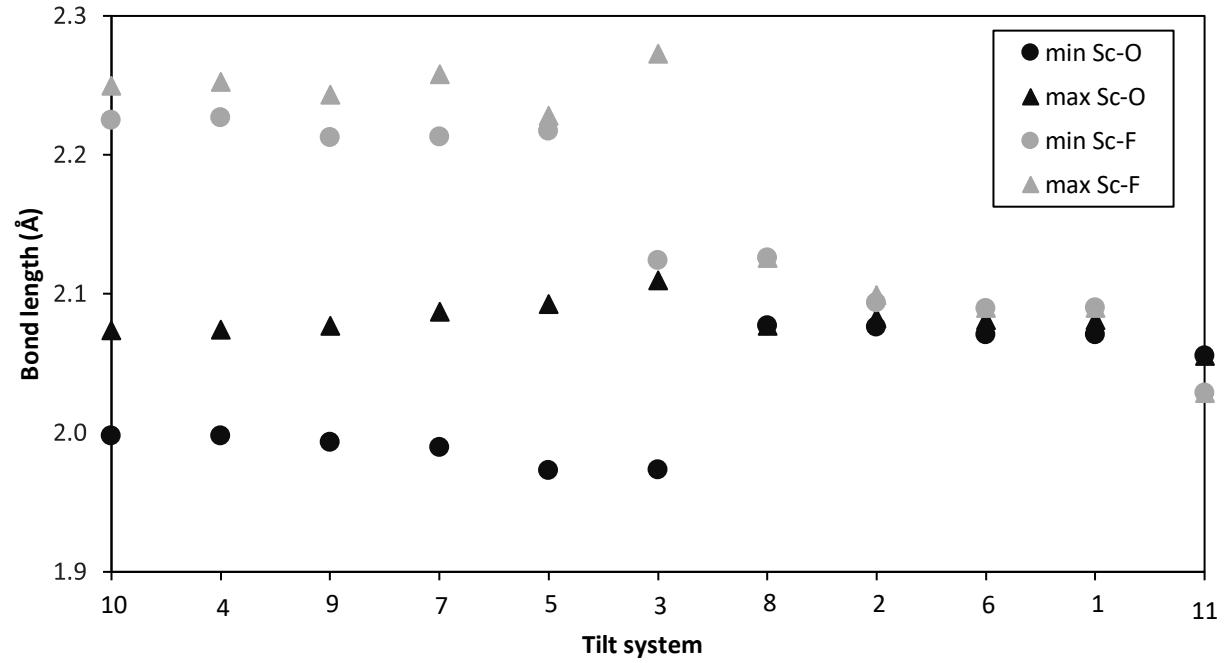
min Sc-O
max Sc-O
min Sc-F
max Sc-F
Bond length (Å)
2.3
2.2
2.1
2.0
1.9
10
4
9
7
5
3
8
2
6
1
11
Tilt system

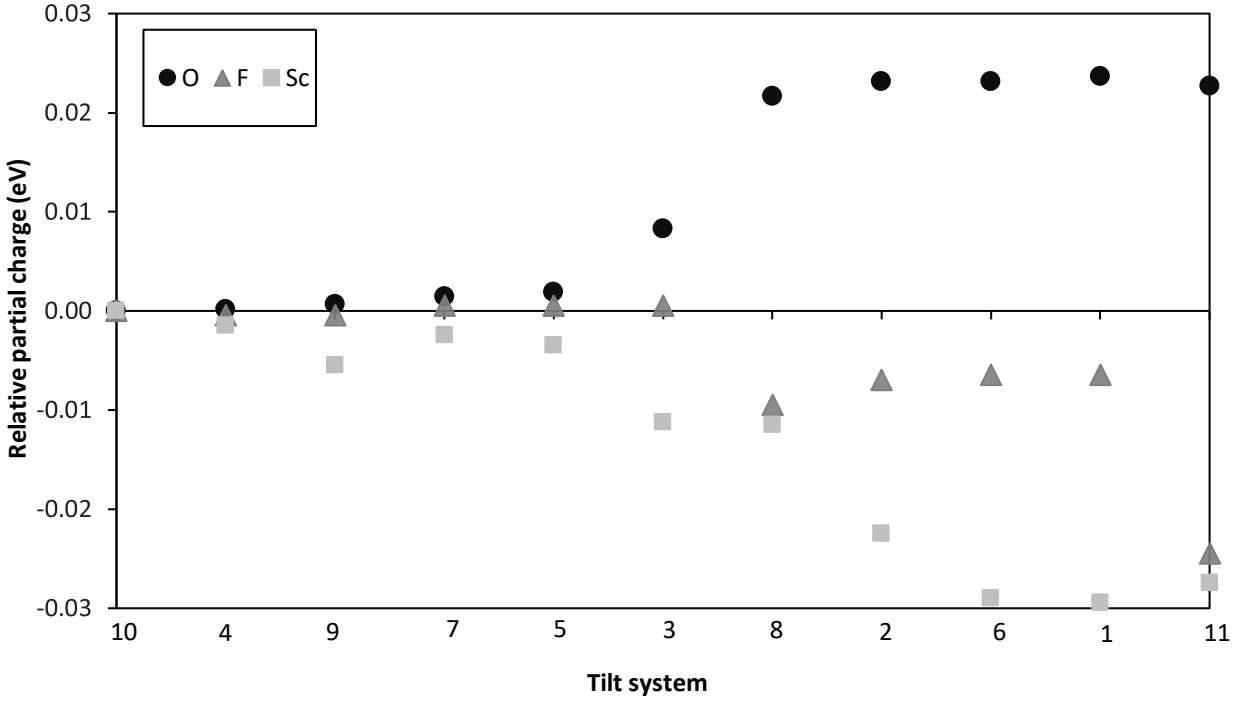
O
F
Sc
Relative partial charge (eV)
0.03
0.02
0.01
0.00
-0.01
-0.02
-0.03
10
4
9
7
5
3
8
2
6
1
11
Tilt system

$KScF_2O$

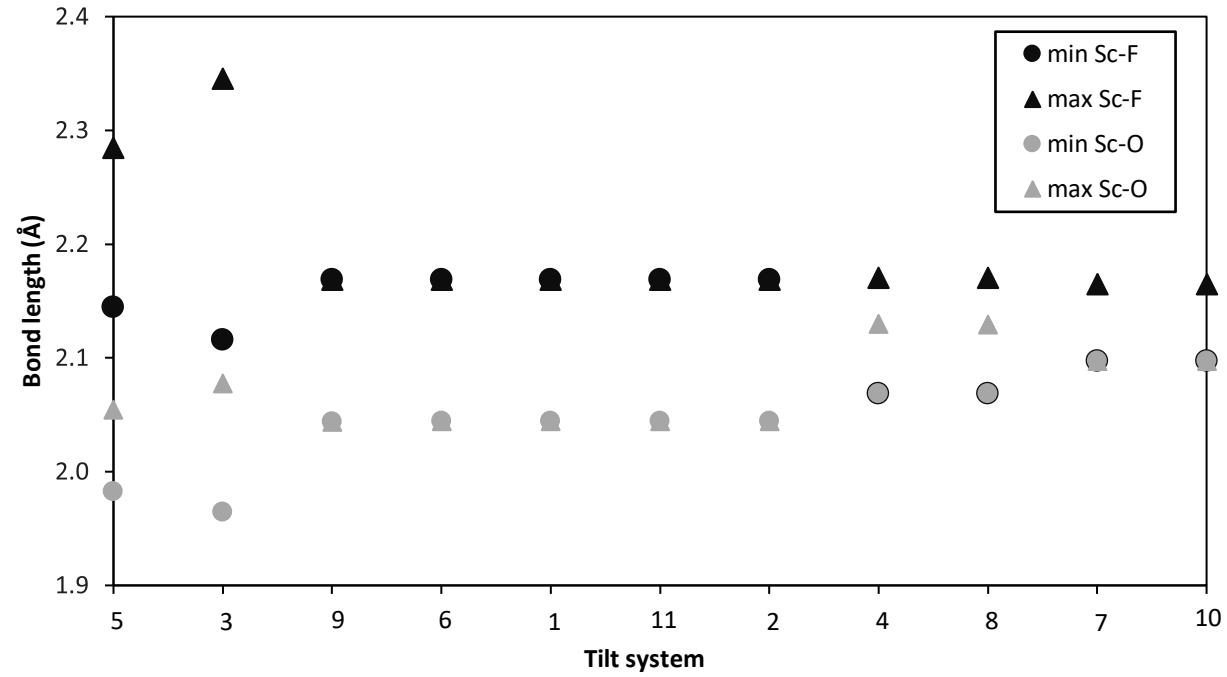
min Sc-F
max Sc-F
min Sc-O
max Sc-O
Bond length (Å)
2.4
2.3
2.2
2.1
2.0
1.9
5
3
9
6
1
11
2
4
8
7
10
Tilt system

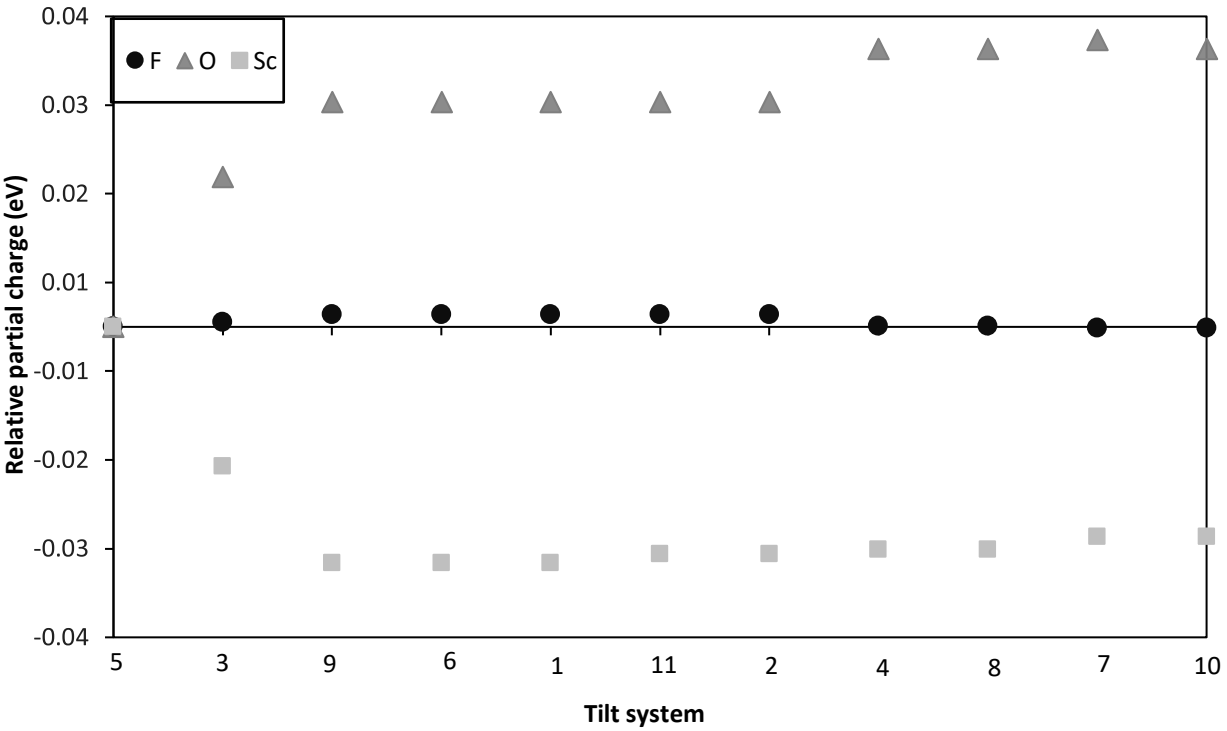
F
O
Sc
Relative partial charge (eV)
0.04
0.03
0.02
0.01
-0.01
-0.02
-0.03
-0.04
5
3
9
6
1
11
2
4
8
7
10
Tilt system

KYF_2O

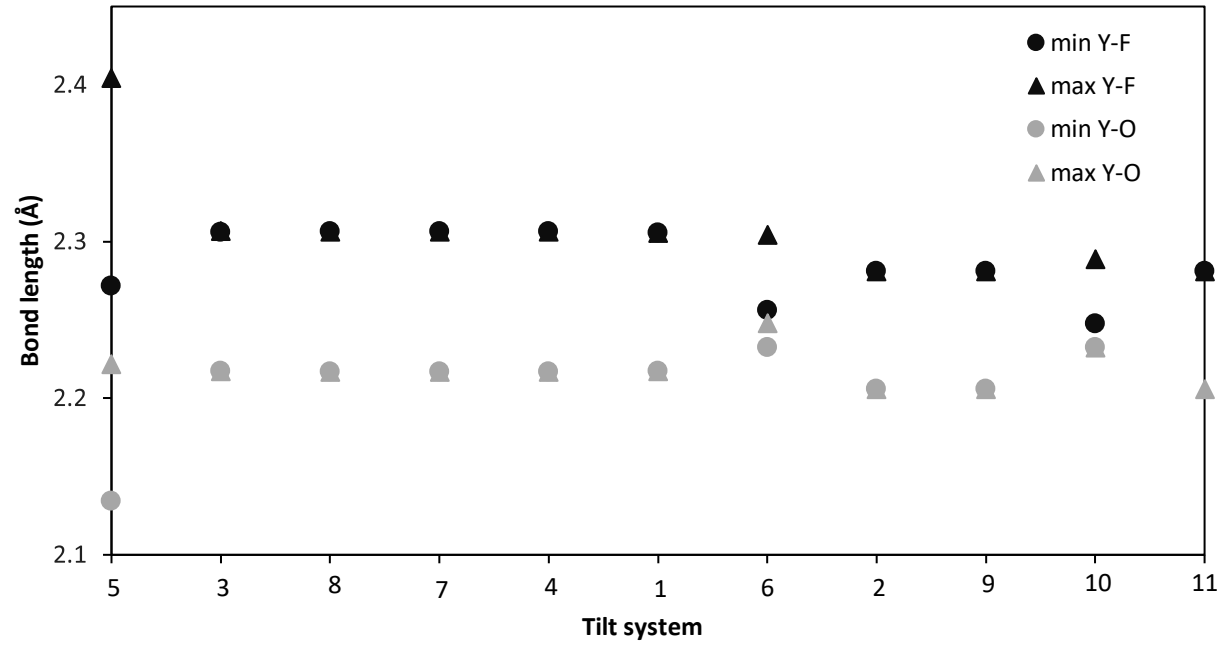
min Y-F
max Y-F
min Y-O
max Y-O
Bond length (Å)
2.4
2.3
2.2
2.1
5
3
8
7
4
1
6
2
9
10
11
Tilt system

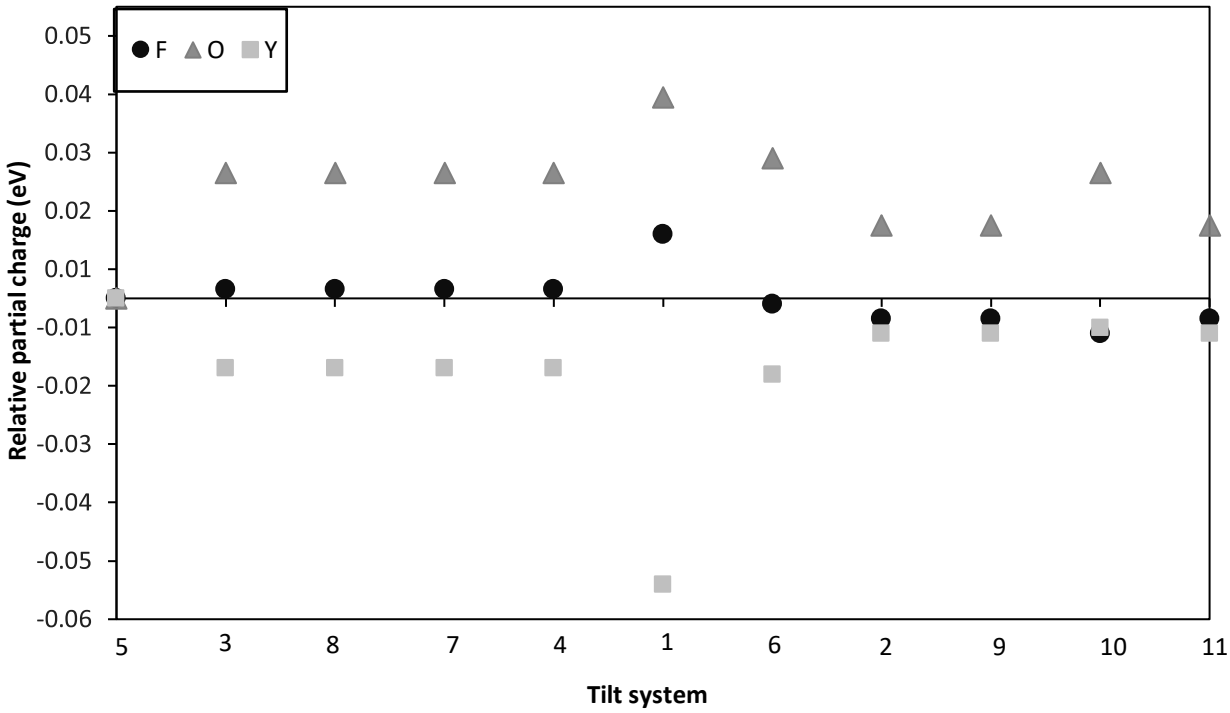
F
O
Y
Relative partial charge (eV)
0.05
0.04
0.03
0.02
0.01
-0.01
-0.02
-0.03
-0.04
-0.05
-0.06
5
3
8
7
4
1
6
2
9
10
11
Tilt system

$NaScF_2O$

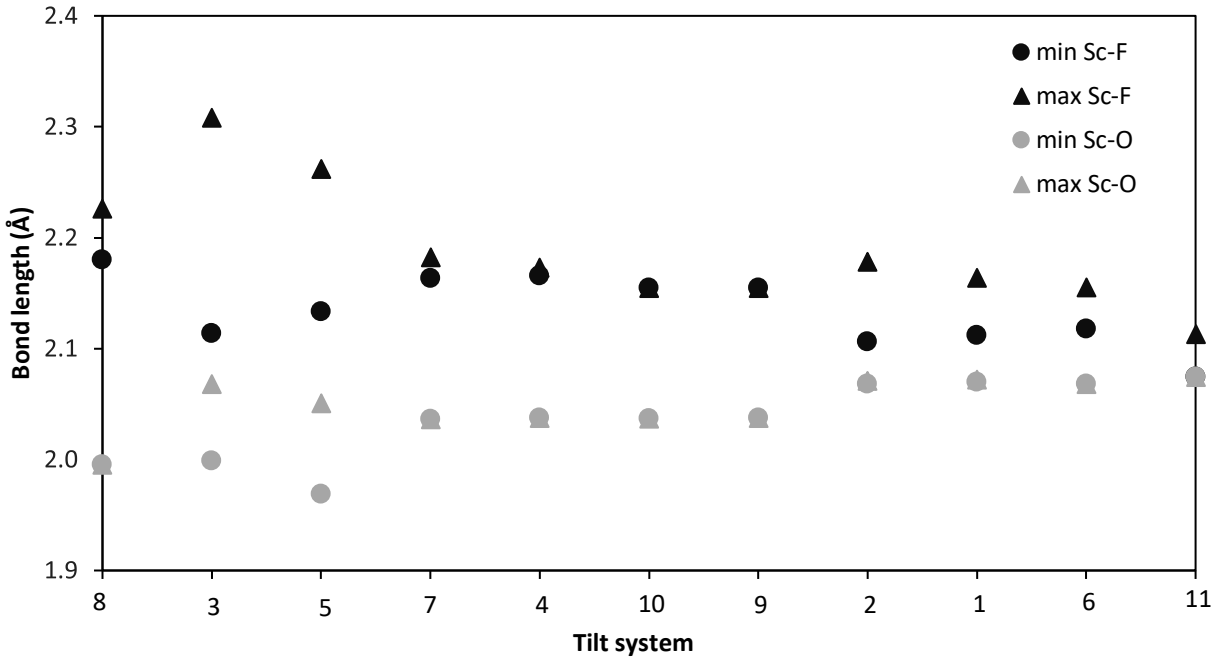
2.4
2.3
2.2
2.1
2.0
1.9
Bond length (Å)
min Sc-F
max Sc-F
min Sc-O
max Sc-O
8
3
5
7
4
10
9
2
1
6
11
Tilt system

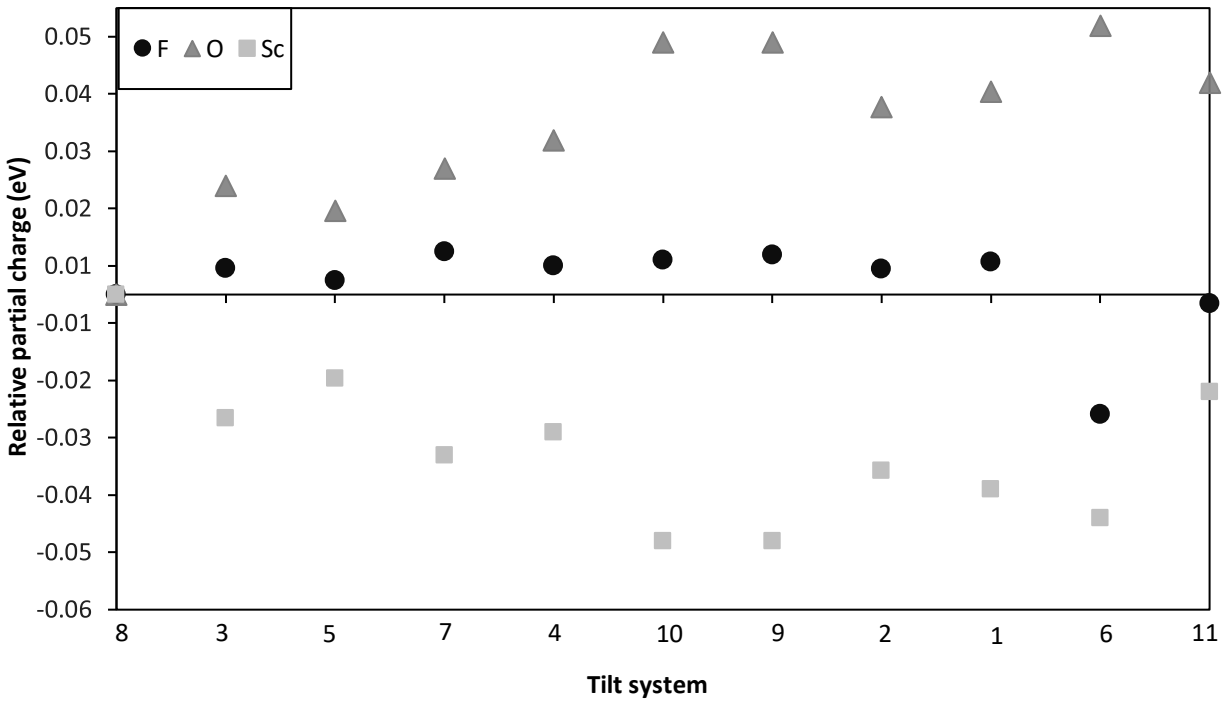
0.05
0.04
0.03
0.02
0.01
-0.01
-0.02
-0.03
-0.04
-0.05
-0.06
Relative partial charge (eV)
F
O
Sc
8
3
5
7
4
10
9
2
1
6
11
Tilt system

$BaNbN_2F$

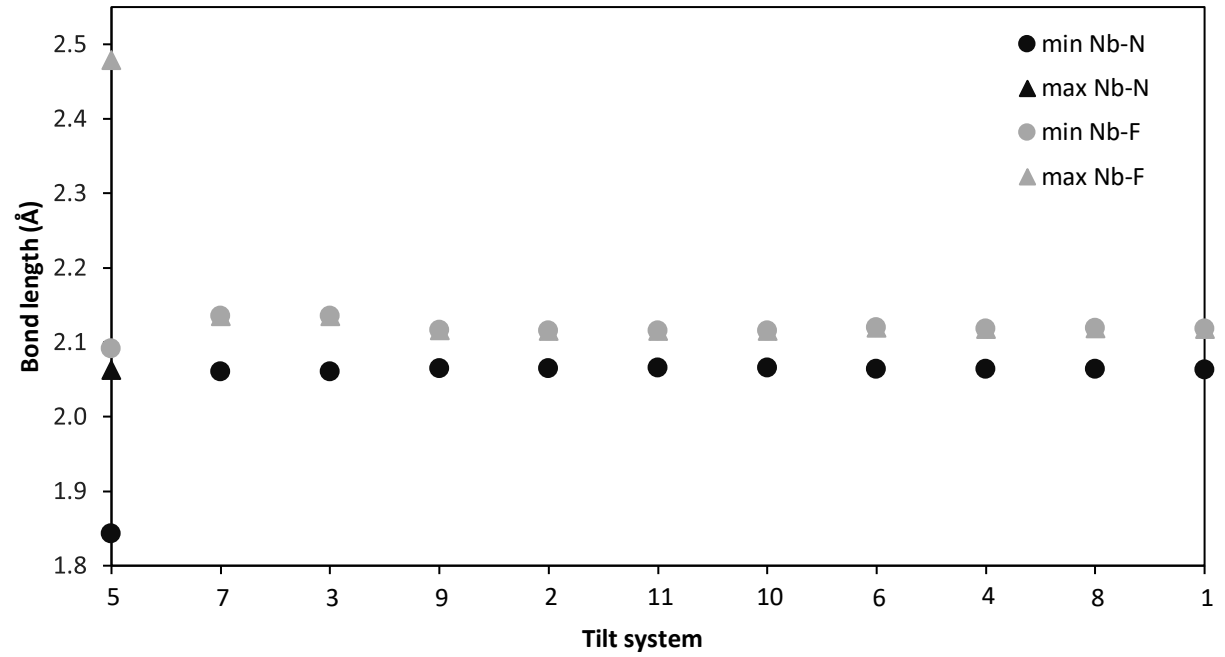
min Nb-N
max Nb-N
min Nb-F
max Nb-F
Bond length (Å)
2.5
2.4
2.3
2.2
2.1
2.0
1.9
1.8
5
7
3
9
2
11
10
6
4
8
1
Tilt system

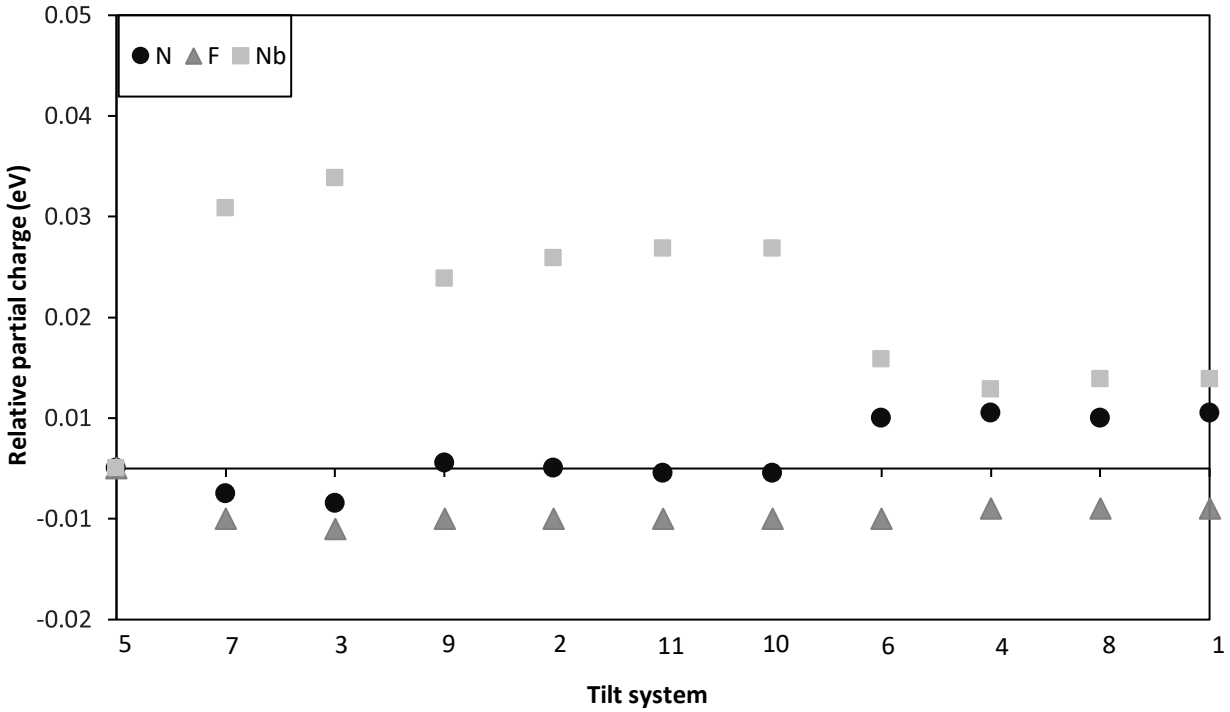
N
F
Nb
Relative partial charge (eV)
0.05
0.04
0.03
0.02
0.01
-0.01
-0.02
5
7
3
9
2
11
10
6
4
8
1
Tilt system

$LaZrN_2F$

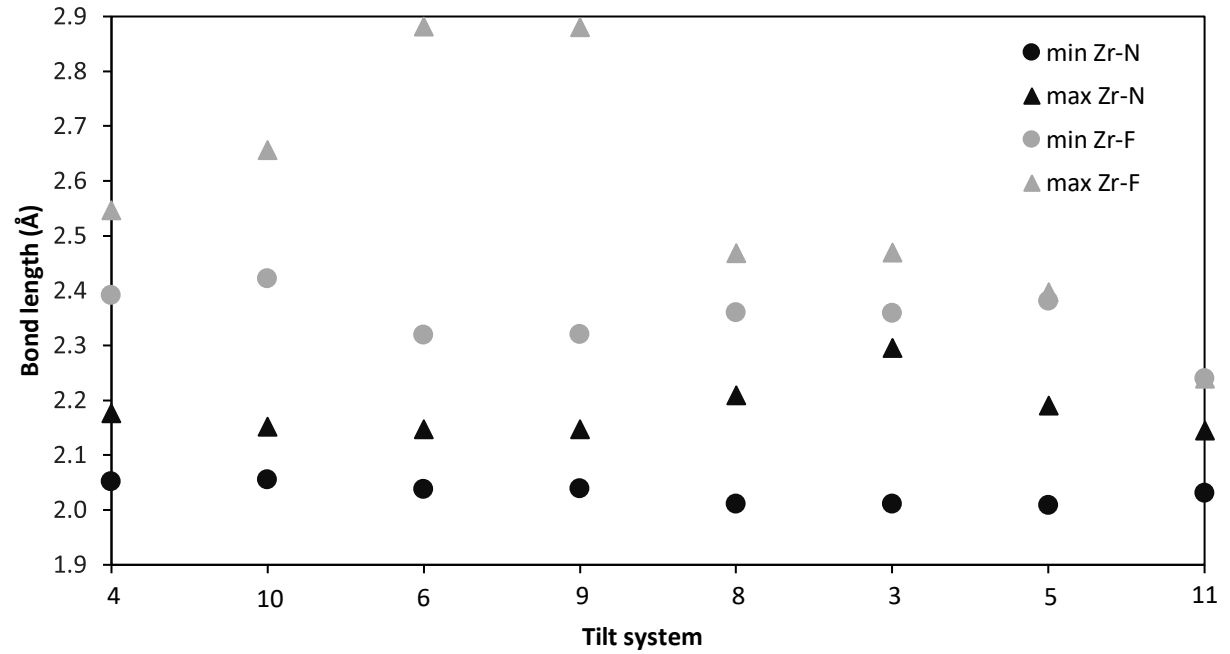
Bond length (Å)
2.9
2.8
2.7
2.6
2.5
2.4
2.3
2.2
2.1
2.0
1.9
min Zr-N
max Zr-N
min Zr-F
max Zr-F
4
10
6
9
8
3
5
11
Tilt system

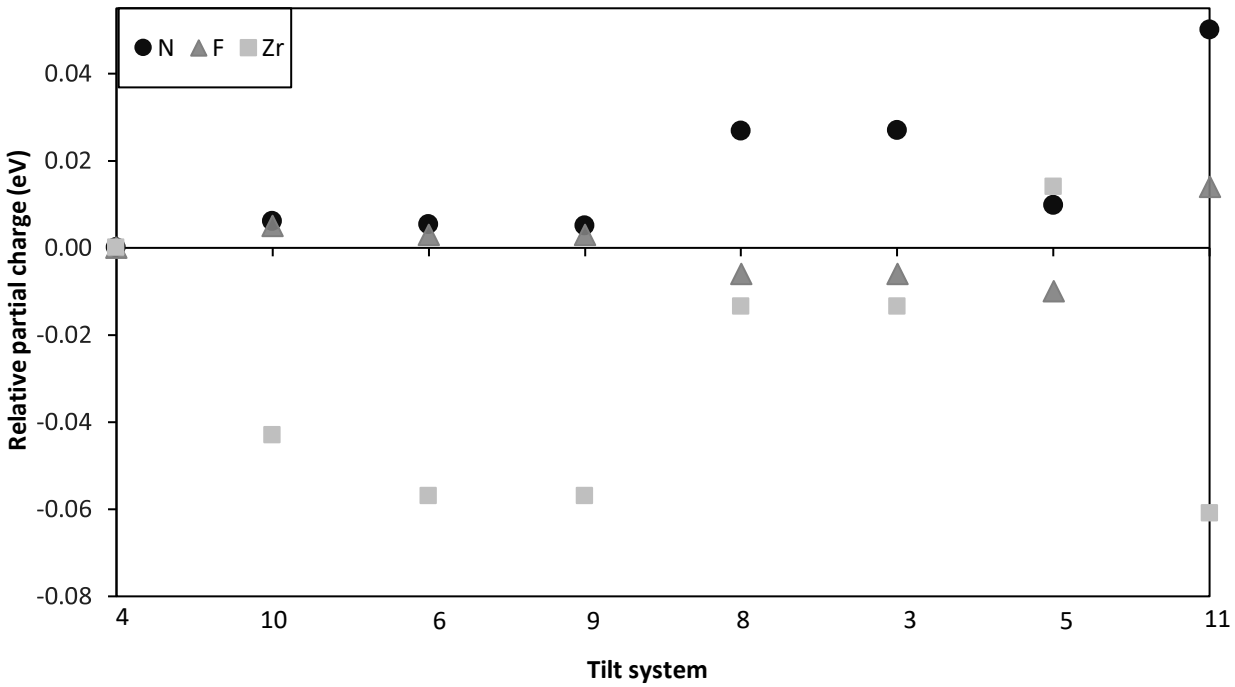
N
F
Zr
Relative partial charge (eV)
0.04
0.02
0.00
-0.02
-0.04
-0.06
-0.08
4
10
6
9
8
3
5
11
Tilt system

$KZrF_2N$

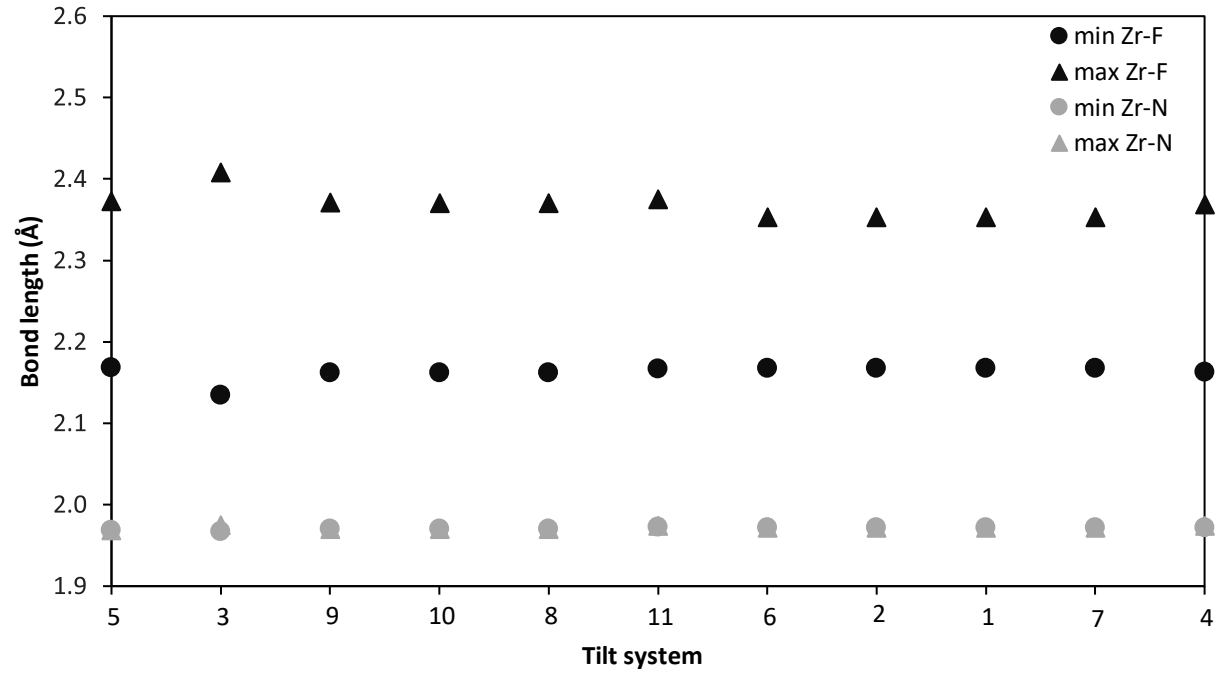
min Zr-F
max Zr-F
min Zr-N
max Zr-N
Bond length (Å)
2.6
2.5
2.4
2.3
2.2
2.1
2.0
1.9
5
3
9
10
8
11
6
2
1
7
4
Tilt system

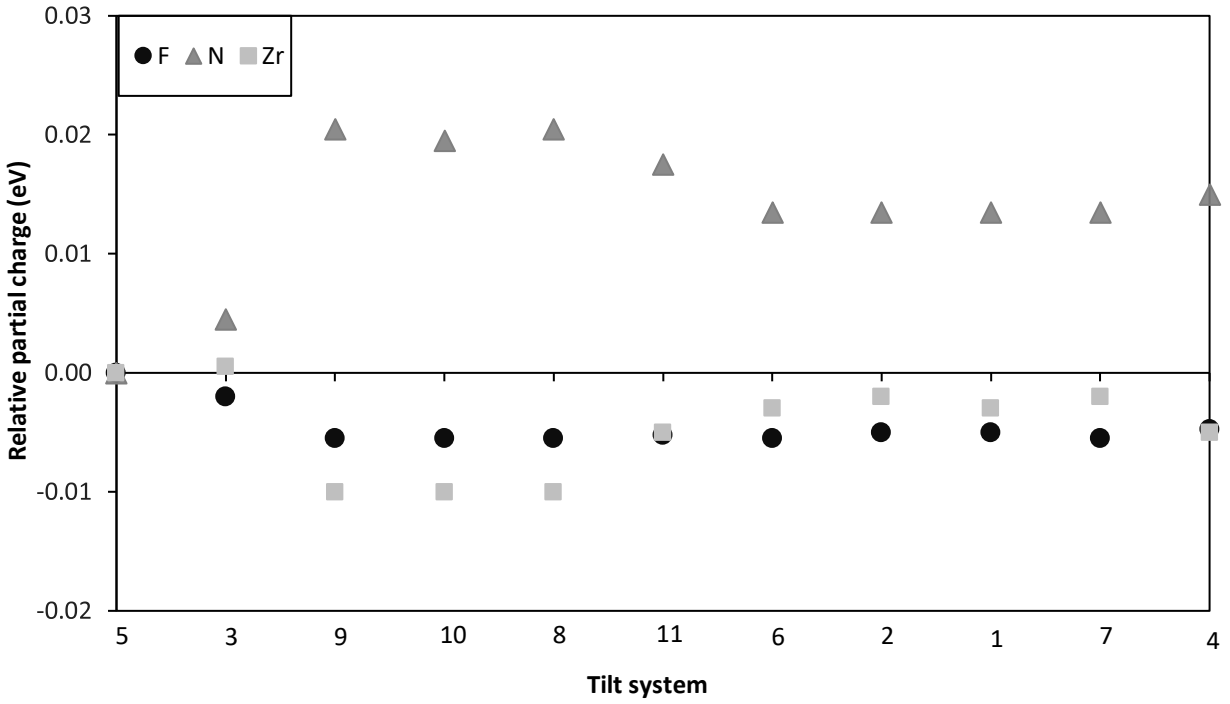
F
N
Zr
Relative partial charge (eV)
0.03
0.02
0.01
0.00
-0.01
-0.02
5
3
9
10
8
11
6
2
1
7
4
Tilt system